A Two-Step Multifrequency Imaging Technique for Ground Penetrating Radar

Alessandro Fedeli, Matteo Pastorino, Andrea Randazzo
Department of Electrical, Electronic, Telecommunications Engineering, and Naval Architecture
University of Genoa, Genoa, Italy
alessandro.fedeli@edu.unige.it, matteo.pastorino@unige.it, andrea.randazzo@unige.it

***Abstract*—In the present paper, a combined method for ground penetrating radar imaging is presented. The proposed technique has a first step in which the electric field scattered by the buried structure is estimated and a qualitative reconstruction is obtained, and a second quantitative inversion step for reconstructing the dielectric properties of the buried targets. The full-wave multifrequency inexact-Newton inversion approach used in the second step uses the information about the target position extracted by the qualitative procedure and takes the scattered field data estimated by a time-domain filtering method. Numerical simulations are presented to prove the effectiveness of the proposed technique.**

***Index Terms*—electromagnetic imaging, Newton methods, buried objects, ground penetrating radar.**

I. Introduction

One of the most challenging problems that arises when trying to obtain quantitative electromagnetic imaging from ground penetrating radar (GPR) data is the reduced amount of available information [1]. Although the ill-posedness and the nonlinearity of the inverse scattering problem are well known [2], [3], in the case of buried object detection we have to deal with several additional factors that make the problem solution more difficult. First of all, the information loss due to the soil attenuation and the uncoupling between soil and antennas. In addition, the usual lack of field probes along several sides of the investigation area. For these reasons, even in very simple cases, conventional microwave imaging approaches may fail. Therefore, in addition to the study of the interaction between antennas and buried structures [4]–[6], there is still the need of devising new inversion techniques in order to use the low available information in a better way [1]. In particular, the combination of more than one imaging methods appears to be attractive, because different techniques can handle different shadows of the same electromagnetic inverse problem [3].

In this period, the scientific community is continuously developing new and interesting approaches for the inverse scattering problem solution [7]–[11]. A rough subdivision of these approaches can be made in qualitative and quantitative techniques. While the first ones aim at reconstructing only specific features of the targets, such as location and shape, the quantitative techniques have the more ambitious goal of the complete electromagnetic characterization of the investigation region [3]. However, in order to exploit the advantages of both kinds of methods, it is possible to combine qualitative and quantitative techniques [12], [13], or extract quantitative information from methods born as purely qualitative [14]. In the present study, we analyze the performances of a combined method composed by a qualitative preprocessing step and a full-wave quantitative inversion obtained by means of a multifrequency inexact-Newton technique [15], [16].

The present paper is organized as follows. In Section II an introduction to the electromagnetic problem is provided, whereas the details of the combined inversion approach are given in Section III. Section IV is devoted to the preliminary validation of the proposed technique with simulated data, and lastly some final remarks are drawn in Section V.

II. Electromagnetic Problem Formulation

The geometry of the electromagnetic problem, which is considered to be two-dimensional, derives from a conventional common offset GPR configuration. As sketched in Fig. 1, we have a bistatic measurement system in which the transmitter and the receiver have a fixed relative offset d and are located at a distance h above the soil level. The observation domain $\mathcal{L}$ is composed by a set of points located on a line of length $L_{\mathcal{L}}$, whereas the investigation domain $\mathcal{S}$ is a rectangle of sides $H_{\mathcal{S}}$ and $W_{\mathcal{S}}$. In this preliminary study, the air-soil interface is supposed to be planar, and we consider a single-layer lower half space, characterized by a dielectric permittivity ϵ_{LS} and an electric conductivity σ_{LS}. The upper half space is air, i.e., with dielectric permittivity $\epsilon_{US} = \epsilon_0$ and a negligible electric conductivity. Frequency domain data are supposed to be available at K different frequencies f_k $(k = 1, \dots, K)$.

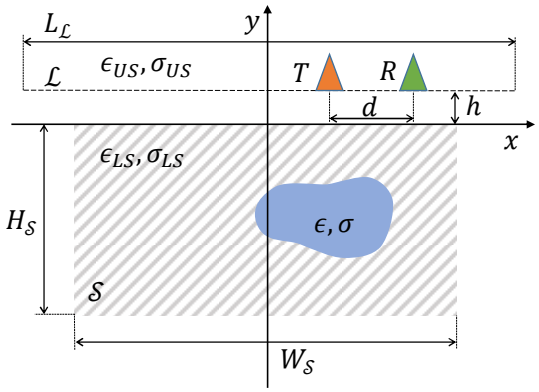

Fig. 1. Measurement configuration and investigation domain geometry.

It is well known that the scattered electric field E_s in frequency domain is given by the nonlinear equation

$$E_s = E_t - E_i = \mathcal{N}_{HS}(x), \tag{1}$$

where E_t and E_i are the total and the incident field, respectively, $\mathcal{N}_{HS}$ is the nonlinear half space scattering operator [3], and x – which is the unknown term in the inverse problem – is a function of the dielectric properties of the investigation domain, i.e., $x = [(\epsilon - \epsilon_{LS})/c_\epsilon \quad (\sigma - \sigma_{LS})/c_\sigma]^T$, being c_ϵ, c_σ normalization coefficients.

III. Two-Step Inversion Method

The objective of the whole inversion method is to find the unknown function x by inverting the relation (1). The approach proposed in the present paper is composed by two distinct steps. The first one is a filtering and qualitative beamforming process, while the second one is a quantitative full-wave inversion obtained by means of an iterative inexact-Newton method [15]. The inexact-Newton method exploits the information found by the preprocessing step, as briefly described in the following.

A. Qualitative preprocessing step

The first step is performed in time domain, combining all the available frequency data by means of the inverse Fourier transform. Let us denote as $e_t = \mathcal{F}^{-1}\{E_t\}$ the time-domain quantity corresponding to the total field, with $\mathcal{F}$ being the Fourier operator. In a practical case, we can measure only the total field, and we have to estimate the field scattered by the buried objects. We can approximate it by properly filtering out from e_t the scattering effects due to the soil interface, obtaining

$$\tilde{e}_s = \Phi(e_t) \tag{2}$$

where $\tilde{e}_s$ is the estimated scattered field, and Φ is a specific filtering operator. Because a simple average removal filter can lead to wrong results and artifacts, we have chosen to use as Φ the adaptive filter designed in [17] for the interface artifact removal step. Once $\tilde{e}_s$ is computed, an estimation of the incident field can be found as $\tilde{e}_i = e_t - \tilde{e}_s$.

Moreover, $\tilde{e}_s$ has been employed in a qualitative technique for locating the buried objects. In our approach, we use a standard delay-and-sum beamforming method in time domain [18] for calculating a normalized target indicator of the cells in $\mathcal{S}$ that may contain the buried targets. Let us denote the obtained normalized target indicator as $\Lambda(\mathbf{r}) \in [0,1], \mathbf{r} \in \mathcal{S}$, that is the result of the beamforming process.

B. Multifrequency quantitative reconstruction

The estimated scattered field $\tilde{E}_s = \mathcal{F}\{\tilde{e}_s\}$ computed in the previous filtering step also forms the known term in the multifrequency quantitative inversion, in which the inexact-Newton algorithm [15] has been employed. Essentially, this algorithm is composed by two nested iterative loops: the outer Gauss-Newton iterations linearize the scattering equation (3), while the inner Landweber steps solve the resulting linear equation in a regularized sense [16]. In the multifrequency version of this approach, all the available frequency samples of the scattered field are used at the same time.

In order to exploit the information about the buried objects position found in the qualitative step, the update of the unknown function $x(\mathbf{r}), \mathbf{r} \in \mathcal{S}$ has been weighted by the normalized target indicator $\Lambda(\mathbf{r})$. The resultant algorithm, presented for the sake of simplicity in case of a single operating frequency, is the following:

1. Linearization of the operator $\mathcal{N}_{HS}$ for obtaining the linear equation

$$\mathcal{N}_{HS}^{x_i} h_i = \tilde{E}_s - \mathcal{N}_{HS}(x_i) \tag{3}$$

where $\mathcal{N}_{HS}^{x_i}$ is the Fréchet derivative of $\mathcal{N}_{HS}$ at x_i.

2. Computation of a regularized solution of the linear equation (3) with respect to the unknown h_i by using the truncated Landweber algorithm [19].

3. Update of the current solution as

$$x_{i+1} = x_i + \Lambda \hat{h}_i \tag{4}$$

where $\hat{h}_i$ is the increment found in step 2 (inner loop).

4. Iteration from step 1 with $i = i + 1$, until a predefined maximum number of outer loop iterations is reached or a proper convergence condition is satisfied.

The algorithm is initialized with an unknown function x_0 that corresponds to an empty investigation domain $\mathcal{S}$. Thanks to the multiplication by the normalized indicator $\Lambda(\mathbf{r})$ in (4), the quantitative reconstruction algorithm is mainly focused on the update of $x(\mathbf{r})$ in the points $\mathbf{r} \in \mathcal{S}$ in which the qualitative procedure has found significant discontinuities with respect to the background properties. Actually, all the cells are updated, but the ones in which Λ assumes higher values (i.e., close to the unity) are updated faster.

IV. Numerical Results

The proposed two-step procedure has been validated with synthetic data. In the considered simulations, the investigation domain $\mathcal{S}$ has dimensions $H_S = 1$ m and $W_S = 2$ m. It has been discretized into 40×20 square subdomains for solving the forward problem with the method of moments [20], and 30×15 cells for the inversion. The medium of the lower half space has been supposed to be dry sandy soil, characterized by $\epsilon_{LS} = 4\epsilon_0$ and $\sigma_{LS} = 0.01$ S/m.

There are two circular cylinders buried in $\mathcal{S}$. The first one, centered at $\mathbf{r}_{c1} = (0.5, -0.2)$ m, has a diameter $d_{c1} = 0.24$ m dielectric permittivity $\epsilon_{c1} = 7\epsilon_0$, and electric conductivity $\sigma_{c1} = 0.01$ S/m. The second cylinder, centered at $\mathbf{r}_{c2} = (-0.35, -0.3)$ m, has a diameter $d_{c2} = 0.16$ m. It is characterized by a dielectric permittivity $\epsilon_{c2} = 8\epsilon_0$, and by an electric conductivity $\sigma_{c2} = 0.02$ S/m. The measurement line of the simulated GPR scan is $h = 0.05$ m far from the soil interface and it is $L_\mathcal{L} = 2$ m long. On this line, $N_\mathcal{L} = 30$ equally spaced measurement positions have been taken into account.

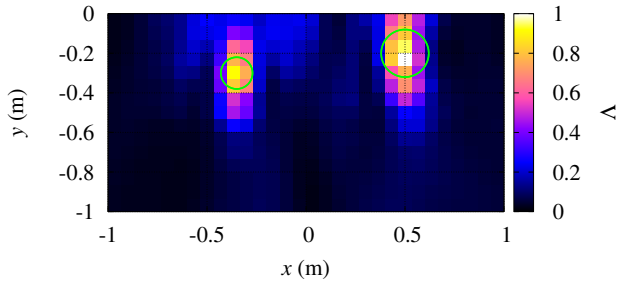

Fig. 2. Spatial distribution of the normalized target indicator Λ in the investigation domain $\mathcal{S}$, for $SNR = 10$ dB.

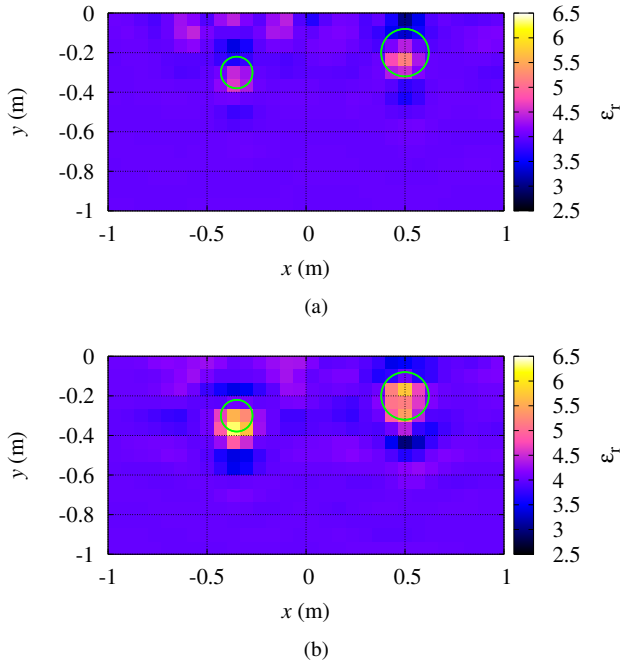

(a)

(b)

Fig. 3. Reconstructed distributions of the relative dielectric permittivity in the investigation domain $\mathcal{S}$ for $SNR = 10$ dB, obtained considering (a) one frequency ($K = 1$), and (b) five frequencies ($K = 5$).

The offset between the transmitter and the receiver is $d = 0.3$ m. For approximating a more realistic environment, a white Gaussian noise with signal-to-noise ratio $SNR \in [5, 30]$ dB and zero mean value and has been added to the scattered electric field data. In the qualitative step, 21 frequencies equally spaced in the band from 150 MHz to 350 MHz have been used. In the quantitative inversion, a subset of K equally spaced frequency samples in the same band have been considered. In the inexact-Newton algorithm, $I = 20$ and $M = 10$ have been used as maximum numbers of Gauss-Newton and Landweber iterations, respectively. The distribution of the normalized qualitative target indicator Λ in $\mathcal{S}$ has been shown in Fig. 2. As can be seen, the location of the two buried cylinders is correctly identified. In Fig. 3 the reconstructed relative dielectric permittivity ϵ_r in the investigation domain is reported. Clearly, the inclusion of more than one frequency ($K = 5$ instead of $K = 1$) allows to obtain better reconstruction

TABLE I

RECONSTRUCTION ERRORS ON THE RELATIVE DIELECTRIC PERMITTIVITY AND ELECTRIC CONDUCTIVITY IN THE BACKGROUND REGION VERSUS THE SNR AND THE NUMBER OF CONSIDERED FREQUENCIES K.

SNR (dB)	$K = 1$		$K = 5$		$K = 9$	
	e_ϵ^b	e_σ^b	e_ϵ^b	e_σ^b	e_ϵ^b	e_σ^b
5	0.016	0.071	0.026	0.069	0.026	0.070
15	0.010	0.048	0.020	0.054	0.020	0.053
30	0.009	0.047	0.020	0.053	0.019	0.052

TABLE II

RECONSTRUCTION ERRORS ON THE RELATIVE DIELECTRIC PERMITTIVITY AND ELECTRIC CONDUCTIVITY IN THE OBJECT REGION VERSUS THE SNR AND THE NUMBER OF CONSIDERED FREQUENCIES K.

SNR (dB)	$K = 1$		$K = 5$		$K = 9$	
	e_ϵ^o	e_σ^o	e_ϵ^o	e_σ^o	e_ϵ^o	e_σ^o
5	0.431	0.434	0.330	0.263	0.317	0.310
15	0.414	0.505	0.311	0.336	0.313	0.310
30	0.414	0.498	0.310	0.351	0.311	0.323

results. The reconstruction performance with different numbers of frequencies included in the quantitative inversion procedure and different signal-to-noise ratios has been studied by analyzing the relative errors on the target dielectric properties, defined as

$$e_a^{R_\mathcal{S}} = \frac{1}{N_{R_\mathcal{S}}} \sum_{\mathbf{r}_q \in R_\mathcal{S}} \frac{\left| a(\mathbf{r}_q) - \hat{a}(\mathbf{r}_q) \right|}{\hat{a}(\mathbf{r}_q)} \tag{5}$$

with $R_\mathcal{S} = \{b, o\}$ being the considered region of $\mathcal{S}$ (background or object, respectively), $N_{R_\mathcal{S}}$ the number of considered subdomains of $R_\mathcal{S}$, $a = \{\epsilon_r, \sigma\}$ the dielectric property for which the error is evaluated, $\mathbf{r}_q$ the position of the qth cell of $\mathcal{S}$, and finally the symbol $\hat{}$ represents the actual value of the considered quantity. In Table I the reconstruction errors related to the background are reported for some values of the SNR and the number of considered frequencies K. As can be seen, the reconstruction error decreases with an increase of the SNR, because with high values of SNR there are less ringing effects in the background region. When the number of included frequencies rises, these error metrics generally increase, as a result of the better visibility of the targets, which causes the presence of small artifacts near them. Furthermore, the reconstruction errors calculated on the objects domain are collected in Table II, versus the SNR and K, as in the previous case. Although these quantities have a greater variability due to the reduced number of cells that belong to the cylindrical targets, it can be noticed that a greater number of frequencies produces a better buried object detection. However, the optimal number of frequencies depends on the target geometry. In this case, with two cylinders of comparable sizes, there is a great improvement in the reconstruction results from $K = 1$ to $K = 5$ frequencies. A further increase in the number of considered frequencies does not have significant effects on the reconstruction performance.

V. Conclusions

A two-step method that combines a qualitative and a quantitative inversion has been presented. The first step is aimed at extracting the field scattered by the object and providing a rough qualitative reconstruction. In addition, a full-wave inexact-Newton technique, which has been modified for exploiting the information acquired by the qualitative procedure, is used for the generation of two-dimensional reconstructions of the buried investigation domain. Future work will include the test of the proposed method with other simulated and experimental data.

Acknowledgment

This work benefited from the networking activities within the EU funded COST Action TU1208, "Civil Engineering Applications of Ground Penetrating Radar."

References

[1] O. M. Bucci, L. Crocco, T. Isernia, and V. Pascazio, "Subsurface inverse scattering problems: quantifying, qualifying, and achieving the available information," *IEEE Trans. Geosci. Remote Sens.*, vol. 39, no. 11, pp. 2527–2538, 2001.

[2] D. Colton and R. Kress, *Inverse acoustic and electromagnetic scattering theory*, vol. 93. New York, NY: Springer New York, 2013.

[3] M. Pastorino, *Microwave imaging*. John Wiley & Sons, 2010.

[4] C. Warren and A. Giannopoulos, "Experimental and modeled performance of a ground penetrating radar antenna in lossy dielectrics," *IEEE J. Sel. Top. Appl. Earth Obs. Remote Sens.*, vol. PP, no. 99, pp. 1–8, 2015.

[5] F. Andre and S. Lambot, "Intrinsic modeling of near-field electromagnetic induction antennas for layered medium characterization," *Geosci. Remote Sens. IEEE Trans. On*, vol. 52, no. 11, pp. 7457–7469, 2014.

[6] S. Šesnić, S. Lalléchère, D. Poljak, P. Bonnet, and K. E. K. Drissi, "Stochastic collocation analysis of the transient current induced along the wire buried in a lossy medium," *WIT Trans. Model. Simul.*, vol. 59, pp. 47–58, May 2015.

[7] M. Salucci, G. Oliveri, and A. Massa, "GPR prospecting through an inverse-scattering frequency-hopping multifocusing approach," *IEEE Trans. Geosci. Remote Sens.*, vol. 53, no. 12, pp. 6573–6592, Dec. 2015.

[8] S. Meschino, L. Pajewski, and G. Schettini, "A SAP-DoA method for the localization of two buried objects," *Int. J. Antennas Propag.*, vol. 2013, p. e702176, Oct. 2013.

[9] I. Catapano, A. Randazzo, E. Slob, and L. Pajewski, "GPR imaging via qualitative and quantitative approaches," in *Civil Engineering Applications of Ground Penetrating Radar*, R. Solimene and A. Benedetto, Eds. Springer International Publishing, 2015, pp. 239–280.

[10] R. Streich and J. van der Kruk, "Accurate imaging of multicomponent GPR data based on exact radiation patterns," *IEEE Trans. Geosci. Remote Sens.*, vol. 45, no. 1, pp. 93–103, Jan. 2007.

[11] R. Persico and F. Soldovieri, "A microwave tomography approach for a differential configuration in GPR prospecting," *IEEE Trans. Antennas Propag.*, vol. 54, no. 11, pp. 3541–3548, Nov. 2006.

[12] M. J. Burfeindt, J. D. Shea, B. D. Van Veen, and S. C. Hagness, "Beamforming-enhanced inverse scattering for microwave breast imaging," *IEEE Trans. Antennas Propag.*, vol. 62, no. 10, pp. 5126–5132, Oct. 2014.

[13] M. Brignone, G. Bozza, A. Randazzo, M. Piana, and M. Pastorino, "A hybrid approach to 3D microwave imaging by using linear sampling and ACO," *IEEE Trans. Antennas Propag.*, vol. 56, no. 10, pp. 3224–3232, Oct. 2008.

[14] L. Crocco, I. Catapano, L. Di Donato, and T. Isernia, "The linear sampling method as a way to quantitative inverse scattering," *IEEE Trans. Antennas Propag.*, vol. 60, no. 4, pp. 1844–1853, Apr. 2012.

[15] C. Estatico, A. Fedeli, M. Pastorino, and A. Randazzo, "A multifrequency inexact-Newton method in Lp Banach spaces for buried objects detection," *IEEE Trans. Antennas Propag.*, vol. 63, no. 9, pp. 4198–4204, Sep. 2015.

[16] C. Estatico, A. Fedeli, M. Pastorino, and A. Randazzo, "Buried object detection by means of a Lp Banach-space inversion procedure," *Radio Sci.*, vol. 50, no. 1, p. 2014RS005542, Jan. 2015.

[17] E. J. Bond, X. Li, S. C. Hagness, and B. D. Van Veen, "Microwave imaging via space-time beamforming for early detection of breast cancer," *IEEE Trans. Antennas Propag.*, vol. 51, no. 8, pp. 1690–1705, 2003.

[18] X. Li and S. C. Hagness, "A confocal microwave imaging algorithm for breast cancer detection," *IEEE Microw. Wirel. Compon. Lett.*, vol. 11, no. 3, pp. 130–132, Mar. 2001.

[19] M. Bertero and P. Boccacci, *Introduction to inverse problems in imaging*. Bristol, UK: IOP Publishing, 1998.

[20] J. Richmond, "Scattering by a dielectric cylinder of arbitrary cross section shape," *IEEE Trans. Antennas Propag.*, vol. 13, no. 3, pp. 334–341, May 1965.